REPORT DOCUMENTATION PAGE

Form Approved
OMB No. 0704-0188

1. REPORT DATE *(DD-MM-YYYY)*: 24-10-2007

2. REPORT TYPE: Final Report

3. DATES COVERED *(From - To)*: April 2007 to October 2007

4. TITLE AND SUBTITLE
Modulated Pulsed Laser Sources for Imaging Lidars

5a. CONTRACT NUMBER: N68335-07-C-0289

5b. GRANT NUMBER

5c. PROGRAM ELEMENT NUMBER

5d. PROJECT NUMBER: 0010203904

5e. TASK NUMBER

5f. WORK UNIT NUMBER

6. AUTHOR(S)
Remington, Scott
Battle, Philip

7. PERFORMING ORGANIZATION NAME(S) AND ADDRESS(ES)
AdvR, Inc.
2310 University Way, Building #1-1
Bozeman, MT 59715

8. PERFORMING ORGANIZATION REPORT NUMBER

9. SPONSORING/MONITORING AGENCY NAME(S) AND ADDRESS(ES)
DCMA Twin Cities
B.H. Whipple Federal building
Room 1150
1 Federal DriveFt. Snelling, MN 55111

10. SPONSORING/MONITOR'S ACRONYM(S): DCMA

11. SPONSORING/MONITORING REPORT NUMBER

12. DISTRIBUTION/AVAILABILITY STATEMENT
Approved for public release; distribution unlimited

13. SUPPLEMENTARY NOTES

14. ABSTRACT
This report summarizes work performed under Navy SBIR topic #N07-036 demonstrating the feasibility of using a pulsed 1064nm laser diode to create pulses at 500 kHz with pulsewidths of 20-25ns that are modulated at RF frequencies using an electro-optic modulator based on engineered nonlinear optical material. The modulated pulses are then amplified using a single-stage fiber amplifier and data is provided showing that powers of 10-15W will be ultimately output. Second harmonic generation from the amplifier output to produce 5W at 532nm is possible using bulk engineered nonlinear optical material. Through the choice of specific laser diode technology, the pulsed output linewidth will remain narrow enough to allow efficient doubling through quasi phase matching while being sufficiently broadened to prevent parasitic processes such as stimulated Brillouin scattering during amplification. The key benefits of this approach include wide latitude in operational pulse rate, pulse width, and modulating RF frequency while remaining in a compact, rugged package.

15. SUBJECT TERMS
laser diode, frequency doubling, fiber laser, fiber amplifier, modulation, pulsed laser, engineered material, electro-optic modulator

16. SECURITY CLASSIFICATION OF: a. REPORT	b. ABSTRACT	c. THIS PAGE	17. LIMITATION OF ABSTRACT	18. NUMBER OF PAGES	19a. NAME OF RESPONSIBLE PERSON / 19b. TELEPHONE NUMBER *(Include area code)*
Unclassified	Unclassified	Unclassified	Unlimited	15	Dr. Linda Mullen (301) 342-2021

SBIR Phase I Final Report

Contract Number: N68335-07-C-0289
Contract Amount: $79,990.00
Navy Small Business Innovation Research Program, Phase I
Title: Modulated Pulsed Laser Sources for Imaging Lidars
Topic: N07-036
Period: 13 April 2007 – 12 October 2007
Security Classification: Non-proprietary

Contractor
AdvR, Inc.
2310 University Way, Building #1
Bozeman, MT 59715-6504
Phone: (406) 522-0388
Fax: (406) 522-0387
Web: http://www.advr-inc.com/

Principal Investigator
Scott Remington
Email: remington@advr-inc.com

TPOC
Dr. Linda Mullen
Email: linda.mullen@navy.mil
Phone: (301) 342-2021
Fax: (301) 342-2030
EO and Special Mission Sensors Division
NAVAIR
Building 2185 Suite 1100-A3
22347 Cedar Point Road Unit 6
Patuxent River, MD 20670

Contracting Office
Karin Weinert
Email: Karin.Weinert@navy.mil
Phone: (732) 323-1177
Fax: (732) 323-2359
Naval Air Warfare Center – Aircraft Division
Code 2.5.2.1.3, Hwy 547, Bldg. 562-3
Lakehurst, NJ 08733-5082

Summary

The overall goal of this SBIR is to develop a compact, highly efficient, RF modulated, pulsed fiber-based laser transmitter at 532 nm for use in the illumination and identification of underwater objects in turbid media. The system consists of a pulsed 1064 nm laser diode whose output is then modulated using an electro-optic beam deflector. The deflector's output is next amplified using a fiber amplifier to an average power of 10-15 Watts. A highly efficient, periodically poled nonlinear optical material will be used to frequency-convert the amplifier output to achieve a minimum of 5 Watts at 532 nm. AdvR fabricates periodically poled materials for efficient pulsed second harmonic generation (SHG) with ongoing research into increasing quality and efficiency. The advantages of the proposed approach consist of variable pulse width, variable pulse rate, and variable modulation frequency with direct RF input.

In this Phase I SBIR, the key objective was to establish the feasibility of both pulsing a 1064 nm laser to produce enough average power to successfully seed a Yb-doped fiber amplifier so it will ultimately produce 10-15 Watts of average power and to investigate the feasibility of using an engineered electro-optic beam deflector with low drive voltage and no bias control as a high extinction amplitude modulator. This report shows the feasibility of the above approach by:

1. Showing that certain laser diodes will meet the bandwidth requirements for pulsing;
2. Showing the modulator will modulate the resulting pulses without suffering from photorefractive damage effects; and
3. Showing that amplification to the power levels necessary to produce 5 Watts of 532 nm light is achievable.

This final report will summarize the activities that took place during the SBIR Phase I Effort "Modulated Pulsed Laser Sources for Imaging Lidars" and present them one subsystem at a time. Finally, a plan will be provided detailing optional interim work to be done if the Phase II effort were funded.

Pulsed Seed Laser

In order to provide variability in pulse rate and pulse width, a fiber-coupled 1064 nm laser diode was chosen as the seed laser. Wavelength stabilization occurs when using Bragg gratings either within the output fiber or within the laser package. When a diode laser is pulsed, its output spectrum is broadened by the current pulse varying the refractive index of the laser cavity that in turn induces a wavelength shift in the output. A small amount of broadening is desired if the output will be amplified to high power by an Yb^{3+} fiber amplifier. If the linewidth remains narrow, stimulated Brillouin scattering (SBS) can occur and will limit the amount of power capable of being extracted from the amplifier. To illustrate this point, the narrowband SBS threshold for the fiber amplifier used in these tests was calculated to be ~20.5 W. When the seed laser output was amplified, the peak power output per pulse was 400 Watts, well above the calculated narrowband threshold implying that linewidth broadening due to pulsing has increased the SBS threshold. This peak power corresponds to an average power of 5 Watts and was obtained before complications due to excessive ASE arose.

While observing the pulsed outputs of several 1064 nm lasers on an optical spectrum analyzer (OSA), it was determined that the narrowest pulsed linewidth occurs when the Bragg grating is closest to the laser diode front facet. The widest linewidth measured was output from a laser

whose grating was placed within the output fiber approximately 1 meter from the laser package. An OSA scan of the narrowest linewidth is shown in Figure 1. The measured linewidth was 0.064 nm, very close to the 0.05 nm resolution limit of the instrument but not instrument limited. The 0.064 nm linewidth equates to $\Delta\nu \approx 17$ GHz in frequency-space implying SBS will not be a major concern while amplifying with 10 μm large mode area (LMA) fiber.

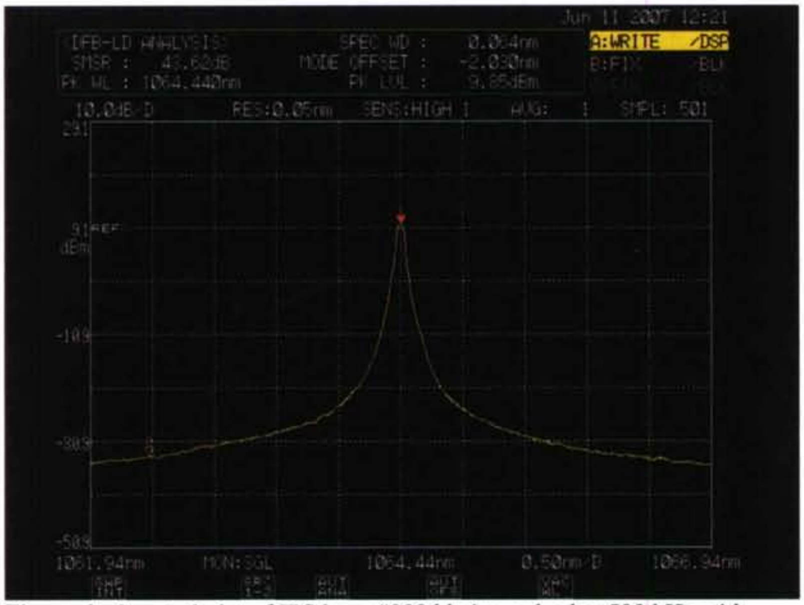

Figure 1. Spectral plot of IPS laser #0886 being pulsed at 500 kHz with Bragg grating next to laser chip within laser package, $\Delta\nu \approx 17$ GHz.

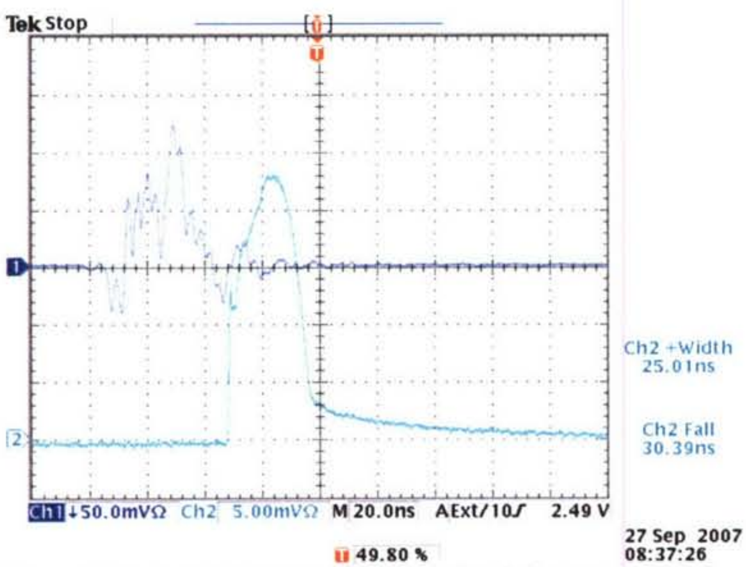

Figure 2. Typical electrical input (blue) and optical output (cyan) of DEI pulsed driver when laser leads are soldered directly to output pads of driver PCB.

Several different pulse drivers from Directed Energy, Inc. (DEI) were used during the testing effort to produce output pulses at 25 ns and 500 kHz. A tail on the trailing edge was noticed during the review of the second bimonthly report and questioned. Because this tail can interfere with the return signal in a lidar system, it was a priority to determine the source of the problem. A typical optical pulse exhibiting the tail is shown in Figure 2 along with a typical current pulse as measured as voltage across a current sense resistor. Tests of different cable configurations and grounding schemes had no effect on eliminating the tail. A driver designed by AdvR personnel around an avalanche transistor for a program with NASA to develop a gain-switched laser was used and eliminated the question whether the problem was with the laser or the driver. This circuit, originally designed to produce 200 ps pulses with Amps of peak current was reconfigured to generate 20 ns pulses by increasing the charge storage capacitance. An example of the resulting optical pulse is shown in Figure 3. While the DEI current pulse could never be sufficiently cleaned up, the pulse output from AdvR's avalanche circuit shows very little noise in comparison (Figure 4).

As Figure 3 shows, there is no hint of trailing-edge tail to be found. This evidence points to the DEI driver as being the source of the tail. Future testing during the option and Phase II would use the AdvR avalanche driver design.

Figure 3. Optical output of laser using in-house gain switching driver circuit that was reconfigured to produce 20 ns pulses instead of 200 ps pulses with Amps of peak current.

Figure 4. Example of current pulse being output from AdvR's avalanche laser diode driver circuit. Very little noise is visible when compared against DEI's output shown in Figure 2.

All pulse testing was done using AdvR's existing 1064 nm laser inventory to see how they perform under pulsed operation. While some effort was spent to extract as much power as possible, none were pushed to the point of failure to see what they ultimately could produce. It is estimated that none of the lasers were driven with more than 2-4 Amps peak current due to double pulsing that started when the DEI driver current was increased above a certain level.

The lasers tested all have maximum CW current levels around 300-400 mA. From a duty cycle standpoint, pulsing with peak currents of 10-20 A if not higher should be possible since the duty cycle is only around 1%. Lasers have been driven to even higher peak currents in other applications[1] which show that this process is commonly used. As laser technology continues to mature, higher power lasers will become more commercially available. One example that directly relates to this effort is a DFB laser[2] manufactured by QPC. This C-mount device has a monolithic semiconductor amplifier allowing the package to output up to 1.5 Watts at 1064 nm with linewidths <0.1 nm. Because this device is capable of such high power CW operation, pulsing with large peak currents should produce outputs higher than what can be obtained from existing laser designs during testing.

---

[1] http://www.hy-line.de/fileadmin/hy-line/power/hersteller/osram/dokumente/Range_finding_using_pulsed_lasers%20HPC.pdf
[2] http://www.qpclasers.com/pdf/products/BLSMSE.pdf

Laser Pulse Modulation

A stoichiometric lithium tantalate (SLT) electro-optic beam deflector developed by AdvR was configured as an amplitude modulator to test the modulation concept. The pulsed seed laser output was collimated and then launched into the modulator crystal. The output of the modulator was then focused into a single mode fiber the output of which was monitored using a 1 GHz photodetector. A 20 MHz function generator capable of outputting 20 V_{pp} was used as the drive source. Sweeping frequency over the generator's frequency range showed little variation in the fiber output except around ~15.5 MHz. In this region, 100% modulation of the transmitted amplitude was observed. Because of the low resonant frequency, a complete modulation cycle cannot be seen in a 25 ns pulse envelope. When the pulsewidth is increased to approximately 120 ns, more modulation cycles are visible as shown in Figure 5. The function generator and pulsed laser driver were operating asynchronously to each other. An individual modulation cycle is displayed in Figure 6 to show that modulation is happening to an optical pulse as the sinusoidal signal can be seen slicing through the relatively fast rise and fall times of the pulse.

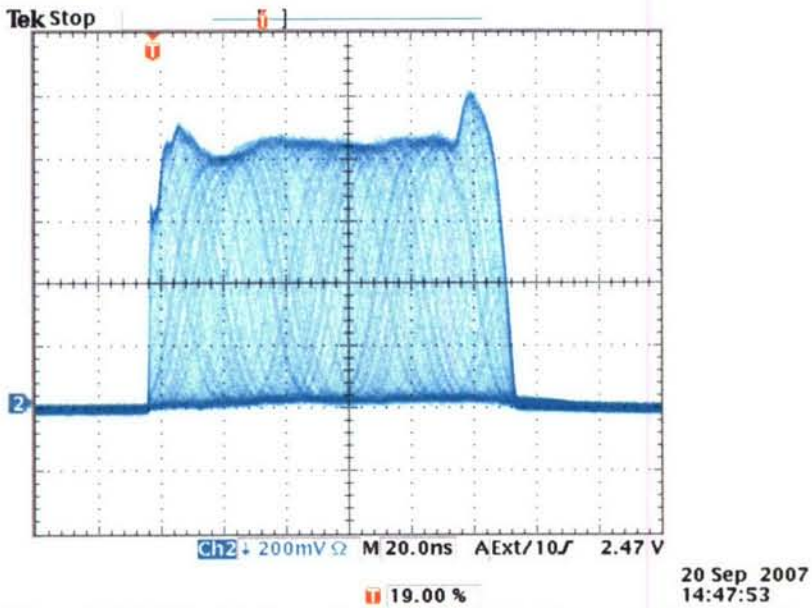

Figure 5. Modulated 120 ns pulse with modulation frequency of 15.45 MHz. Asynchronous operation of function and pulse generator.

Maximum extinction at resonance occurred with a function generator output of ~10 V_{pp}. Lower voltages would reduce the extinction ratio while voltages up to 20 V_{pp} would overdrive the modulator and result in reduced extinction ratios as well. Shortening the wire lengths used to make electrical connections to the crystal did not result in any appreciable change to the resonant frequency.

The modulator used for these tests is based on the same electro-optic material used by other companies such as Conoptics or Leysop who produce bulk modulators with modulation frequencies in the hundreds of MHz. The difference lies in how the crystal is configured for modulation. Other amplitude modulators typically rely on operating their devices like a Pockels cell where the applied RF voltage imparts a polarization rotation onto the incident light. To

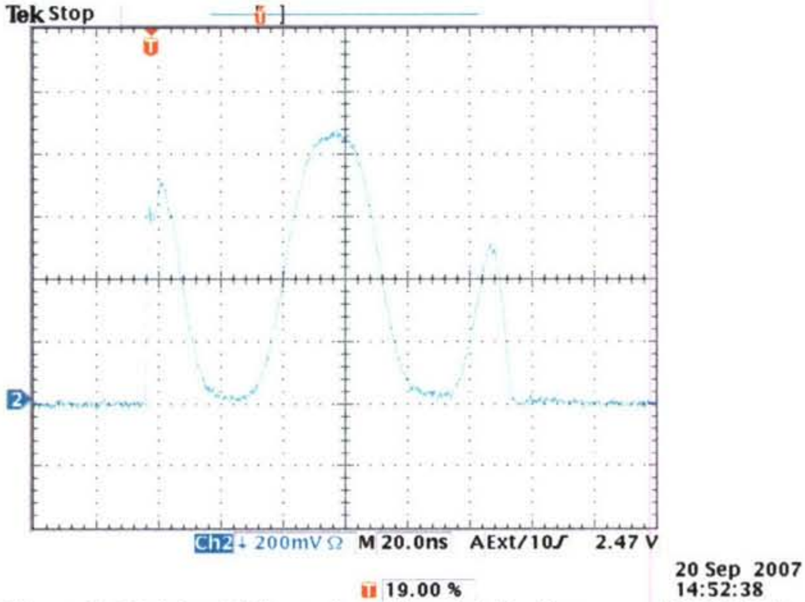

Figure 6. Modulated 120 ns pulse with modulation frequency of 15.45 MHz showing modulation cycle within pulse during a single shot.

ensure best extinction, these modulators typically require adjustment of a bias voltage to compensate for environmental drift. In the AdvR design, the applied RF voltage causes the incident light to be physically deflected away from its zero voltage direction. Engineering the pattern within the crystal to maximize deflection of the beam ensures best extinction.

In order to drive these crystals with RF energy up to 1 GHz, complicated but understood impedance matching techniques must be used. Otherwise, RF issues such as mismatched feedlines and impedances will prevent efficient modulation. While these techniques must be applied to the AdvR-developed modulator as well, the AdvR approach has several distinct advantages that reduce the matching effort needed. By using better materials with higher damage thresholds, smaller spot sizes can be used within the modulator package without causing damage. By using smaller spot sizes, smaller clear apertures and smaller crystals can be used which have the benefit of reduced drive voltages (reduced cross-section so same electric field strength is possible with lower applied voltage) as well as higher frequency operation due to reduced capacitance in the smaller crystal.

To measure the amount of impedance mismatch, the modulator was tested using a network analyzer. Its impedance was measured from 100 MHz to 1 GHz in three different configurations – without 50-ohm terminators and with 50 ohms in series and in parallel. The measurements, in the format of standing wave ratio (SWR) are shown in Figure 7. It is not a complete surprise that the unterminated crystal shows large SWR values since it is acting like a capacitor (a short) to the supplied RF energy. Even when terminated with a 50 Ω parallel load, system response is still greater than 1.5:1. The region where SWR <1.5:1 is shown in Figure 7 as the area at the bottom of the graph between the two dashed lines. This is important to note because the vast majority of commercial RF equipment like transmitters, amplifiers, etc. require a load impedance between 33 and 75 ohms to prevent the equipment from being damaged and to ensure maximum power transmission.

The ultimate goal of the modulator design is to develop a device with an upper end frequency of a minimum of 800 MHz. Being able to modulate beyond 1 GHz would be beneficial but not required. These frequencies are approaching the microwave region where the modulator itself and its electrodes can no longer be considered parts of a lumped circuit. A transmission line analysis will probably be required where the electrode (crystal) width and spacing (crystal thickness) must be optimized for a 50-ohm impedance. During the optimization process, it may be discovered that to get the correct impedance, the crystal thickness must be reduced by half. This would have the effect of reducing the required voltage by a factor of two, or if the voltage is acceptable as-is, the crystal length may be cut in half to reduce capacitance and the light double-passed through the crystal to get the same deflection.

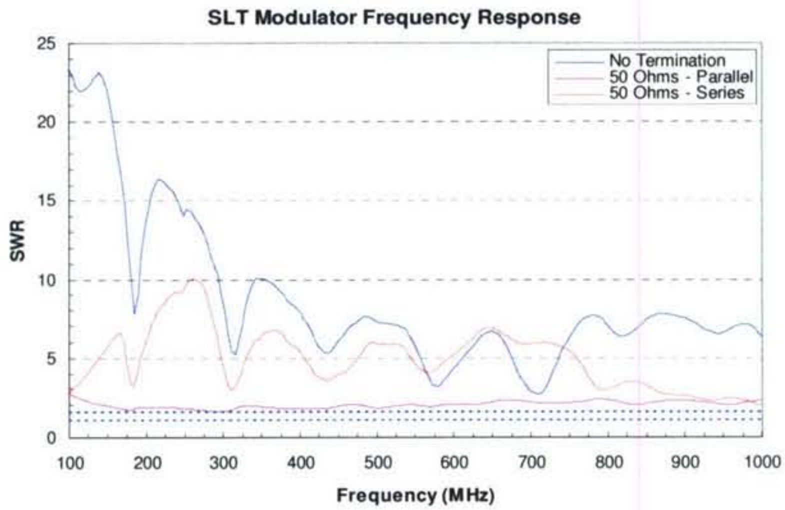

Figure 7. Frequency response of tested SLT modulator unterminated and terminated with 50 ohms. The impedance mismatch is very large in almost all situations resulting in radiation from the feedline and a high percentage of incident power being reflected back from the modulator.

To verify the model's ability to predict modulator performance, beam deflection was measured with a DC bias voltage. A whole-beam deflection of 6±1 mrad was measured while the theoretical deflection for the given voltage and beam parameters was 7 mrad. From these measurements, the modulator and model were performing as expected and the model is in good agreement with measurement. Because there is nothing in the model that is frequency dependent, performance at RF frequencies should not be a concern, as long as correct impedance matching is done.

The modulator model has shown that it can correctly predict performance as evidenced by the amount of deflection resulting from a given applied voltage matching within experimental error the value measured in the laboratory. This model has predicted that a 1 mm thick and 2" long modulator fabricated from either MgO:SLT, MgO:LN, or KTP will provide enough deflection to force the light out of the core of an optical fiber that it has been focused into. An optimized design for a low drive voltage, fiber coupled, electro-optic amplitude modulator developed from the model is shown in Figure 8.

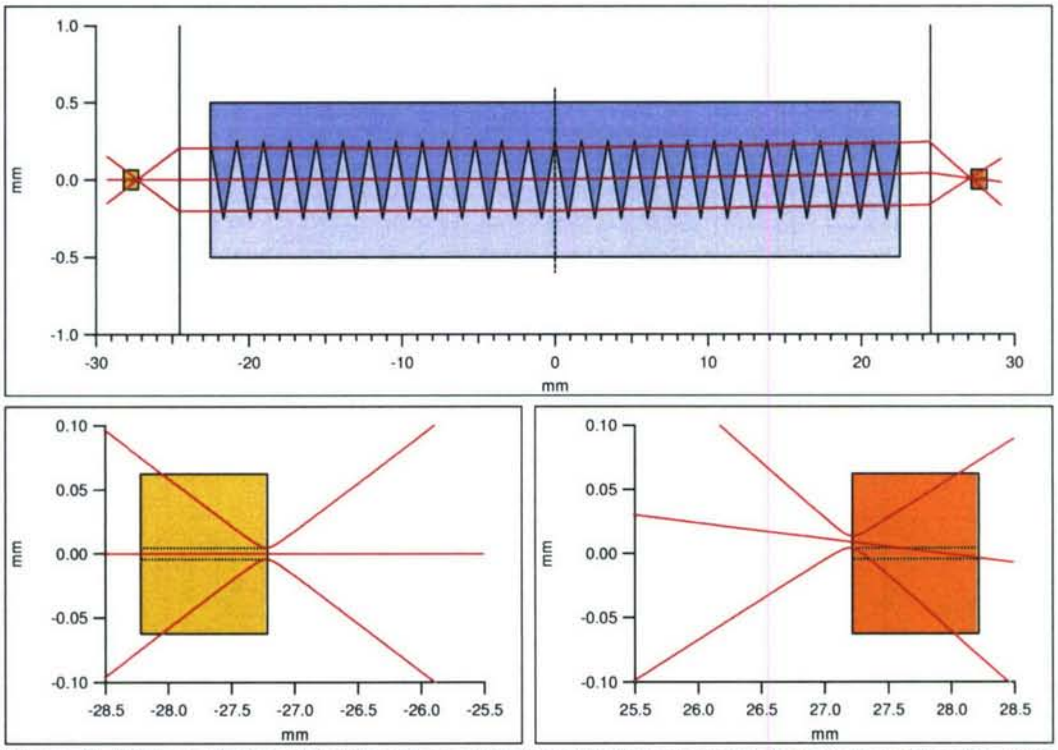

Figure 8. Mathematical model of the fiber coupled amplitude modulator. Beam propagation from left to right is shown for a given drive voltage of 25.2 V. $1/e^2$ beam diameter is plotted in red.

The top picture in Figure 8 illustrates the overall modulator concept with light being collimated as it exits a single mode fiber on the left. After being collimated, it is incident on the modulator input face normal to the surface. After traversing the entire crystal length, the beam has been deflected enough so that when focused and launched into another single mode fiber, the image spot on the fiber face misses the fiber core and no light is transmitted. The left hand bottom picture illustrates the collimation geometry on the input side of the scanner. The right hand picture illustrates how the refocused beam exiting the modulator just misses the fiber core. If the modulator was configured in a double-pass style instead of single-pass as shown in Figure 8, the required drive voltage can be reduced by a factor of two, or the length can be shortened by a factor of two. Both of these actions would result in an increase in the frequency response. By reducing the voltage, the usefulness of a frequency generator or amplifier could possibly be extended into its rolloff region. By reducing the length, the capacitance is reduced again allowing for higher frequency operation.

<u>Preliminary Fiber Amplifier Testing</u>

The proposed system design requires an Yb^{3+} fiber amplifier capable of producing 10-15 W of polarized, quasi-CW output at 1064 nm that would then be converted to 5 W at 532 nm using a periodically poled nonlinear material. To test the feasibility of using a single stage amplifier, efficiency tests using an existing 16 W fiber amplifier were performed.

Single stage amplification is preferred because it reduces system complexity by not requiring dual sets of pump lasers and their associated control electronics. In addition, the requirement for

isolators and ASE filters is removed when a single stage amp is used, again reducing system complexity. The amplifier test bed used is shown in Figure 9 and is comprised of a 3 meter length of 10/125 μm dual-clad Yb^{3+}-doped PM fiber. The ytterbium ions in the fiber are cladding-pumped to their excited states using four, 6-Watt multimode lasers at 976 nm.

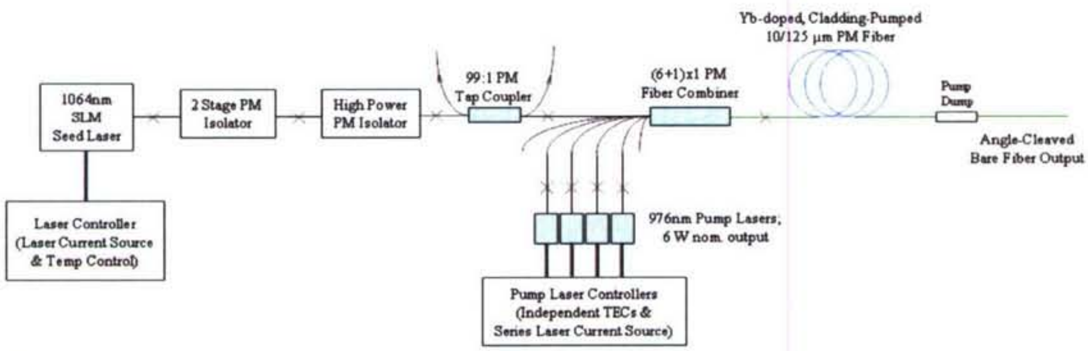

Figure 9. Single stage Yb^{3+} fiber amplifier configuration being used to amplify pulsed seed laser output.

Using the DEI driver, average pulsed seed power into the amplifier was approximately 4 mW after isolator losses. Amplification resulted in a maximum of 5 Watts being output before the test was terminated. Termination resulted due to the loss of three out of four pump lasers from front facet damage with still no sign of rolloff in the output power which would typically be the sign of approaching or exceeding the SBS threshold. This damage was caused by the refocusing of backward-propagating single mode light onto the pump laser chip by the fiber-coupling lens. In this situation, the single mode light is very tightly focused causing the surface of the semiconductor material to become damaged and converting the laser diode into an LED. At the point of failure, almost 800 mW of backward-propagating light was being measured. When this amplifier is operated in normal CW fashion at the 15 W level, backward power is typically no larger than 200-300 mW. The two to four times increase and laser damage are direct results of the low input seed power and very high amplifier gain (>32 dB). With higher seed powers, amplifier gain will be reduced to more sustainable levels and create a more stable output.

Before damage occurred, the amplifier's spectral output was measured at 1.7 W. Spikes in the amplified spontaneous emission were beginning to show around 1040 nm. This is typically a sign that different wavelengths are competing for amplifier gain and as the pump levels are raised, these spikes may dominate output and force a reduction of power at 1064 nm. An OSA plot of this condition is presented in Figure 10. This behavior is a typical example of when an amplifier is not being driven into saturation and pumped with excess power. When an amplifier is operated with a saturated input, relatively large changes in input do not affect the output in anything more than small changes. On the other hand, when an amplifier is not saturated, small changes in input power result in relatively large changes in output. This can be seen in a model of the CW amplifier output vs. seed input in Figure 11.

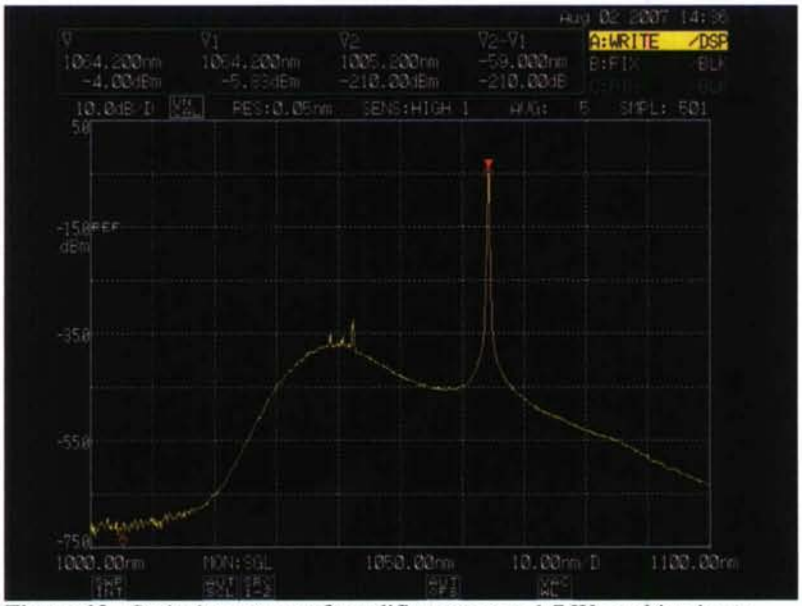

Figure 10. Optical spectrum of amplifier output at 1.7 W resulting in an amplifier gain of 28 dB. Excessive amplifier gain is causing the background spontaneous emission around 1040 nm to become amplified. Increased seed input will suppress ASE while increasing amplifier output at the seed wavelength.

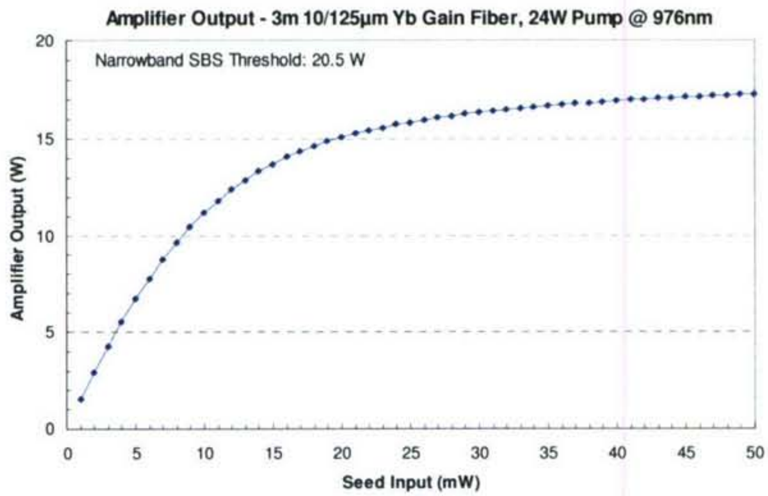

Figure 11. LAD model of CW amplifier output using 3 meters of 10/125 µm Yb-doped gain fiber showing the effect of amplifier saturation.

As the graph in Figure 11 shows, with a fixed pump power, the higher the seed input power, the higher the amplifier output and the more stable the output will be to input power fluctuations. The model was close to predicting the output actually being measured before damage occurred. This implies a seed power of 20 mW will produce an output around 15 W. For additional amplifier power, increasing the seed produces diminished gains. Increasing the pump power will allow higher outputs without affecting the SBS threshold. Increasing amplifier fiber length will

allow for higher outputs, but at the expense of reducing SBS threshold. For example, increasing the 3-meter fiber length to 4 meters with the same 24-Watt pump input and 50 mW seed input will reduce the SBS threshold from 20.5 W to 15.4 W while only providing roughly 700 mW of additional output power. Luckily, when the seed laser is pulsed, its linewidth will increase as shown earlier which will raise the SBS threshold and allow for additional power extraction. To conclude this section, both testing and modeling show that increasing seed powers are essential to having a feasible single stage amplifier design. Driving existing style lasers with higher peak currents using the avalanche transistor circuit developed by AdvR should provide seed powers capable of amplifier saturation. If not, lasers such as the QPC product should provide the required seed powers simply by pulse slicing. If seed powers still cannot saturate an amplifier, multiple stage amplification can be considered. When doing this, high output powers are certainly possible, but at the expense of increased system complexity.

Second Harmonic Generation

No work has been performed regarding second harmonic generation as per the work plan provided in the Phase I proposal. From past tests, a conservative conversion efficiency of 30-50% should be possible with bulk poled nonlinear materials when used with pulsed sources. As stated in the Phase I proposal, one of the tasks defined under the Option would be to model SHG using the beam parameters measured for this Phase I project. This would still be a viable task if the Option were authorized.

Option Work Plan

Task 1: Pulse a 1064 nm DFB laser from QPC and IPS and measure their spectral properties and average power. Using a pulsed driver based on the avalanche transistor circuit being used for gain switching, a 1064 nm DFB laser manufactured by QPC and a DBR-style laser from IPS will be driven at 500 kHz with a nominal pulsewidth of 25 ns. The average output power will be measured as a function of oscillator current and amplifier current. The spectral content of the output will be measured using an optical spectrum analyzer with a resolution of 0.05 nm. This information will be used to refine the amplifier model generated in Task 2.

Task 2: Establish an amplifier design capable of achieving the specified performance levels. Existing fiber modeling software and the results from Task 1 will be utilized to develop a 1064 nm Yb-doped amplifier design whose output will be appropriate for subsequent generation of the required 5 W of pulsed 532 nm light. The model will establish the key amplifier parameters including fiber length, dopant level, fiber core/cladding size and pump power, as well as provide estimates on the magnitude of ASE and SBS within the modeled amplifier.

Task 3: Use existing software to establish a crystal configuration that is capable of achieving the specified performance for efficient single pass SHG. Modeling using SNLO will be implemented for optimizing the crystal length and confocal parameters to achieve high efficiency conversion for specific pulse rates and pulsewidths. Crystal size will be determined by using photorefractive (PR) damage and catastrophic optical damage (COD) thresholds as constraints on the upper limit of input fluence. A choice will be made between PPKTP and PPSLT to use the most efficient crystal for this application.

Conclusions

The main tasks of this Phase I SBIR program were to obtain performance data from several pulsed laser diodes operating with nominal pulse widths of 25 ns and pulse rates of 500 kHz and then modulate those pulses using an existing modulator crystal. This information would then be used to develop a fiber amplifier model and a frequency doubler model that allows for an average power of 5 Watts of 532 nm light whose pulses can be modulated up to 800 MHz. The questions to be answered included the following:

1. How much average power can be obtained from a pulsed laser at these pulse parameters? Is this power sufficient to seed a single stage fiber amplifier for an ultimate output of 10-15 Watts?
2. How much linewidth broadening occurs when these lasers are pulsed? Is the broadening wide enough to increase SBS threshold while remaining narrow enough to remain within the acceptance bandwidth of the SHG crystals being considered?
3. Can an electro-optic amplitude modulator be designed to provide a minimum of 90% extinction of the modulated beam while minimizing the drive voltage?
4. Will photorefractive effects be a concern for the modulator at the expected powers being output from the seed laser?
5. How does an existing modulator crystal perform when compared to the design model and how does this crystal perform when modulated at RF frequencies?

Based on the duty cycle and the maximum CW drive current recommended for this class of laser, pulsing with peak currents much higher than was tested should result in higher average output powers with much higher single pulse peak powers. These outputs could very well be at the saturation level. If, however, other issues prevent the output from increasing to what is expected, other lasers are commercially available now that may provide the needed power. An example of such a laser is the QPC C-mount monolithic oscillator/amplifier which can output 1.5 Watts CW. Simply derating the CW power by the duty cycle of 1.25% (25 ns divided by 500 kHz pulse period of 2 μs) shows that 18 mW should be achievable. Pulsing at slightly higher currents should allow for higher average powers that in turn will compensate for optical losses before the amplifier. In the unlikely event average power is still not high enough to meet the needed 1064 power, a preamplifier stage can be employed so the gain in the main amplifier does not need to be so large. These amplifiers can either be purchased components or built in-house.

When the Bragg grating is kept as close as possible to the laser diode, pulsed linewidth broadening is reduced but is not as narrow as when run in CW mode. Measurements of existing lasers indicate that pulse broadening results in linewidths less than 0.07 nm. This broadening seen is still less than the 0.2 nm maximum acceptable linewidth for doubling with periodically poled materials so second harmonic generation should not be adversely affected. Computer modeling predicts the CW narrowband SBS threshold for the fiber amplifier used in testing to be around 20.5 W. Even at the 5 W average power output seen with the approximate 5 mW seed input, SBS rolloff was not seen. Peak power levels in this configuration were 400 W, almost 20 times the CW SBS threshold. Therefore, linewidth broadening should be adequate to reduce the effects of SBS in the amplifier.

Modeling has shown that a 2" long, 1 mm thick SLT or LN modulator will deflect the focused beam away from the core of a single mode fiber and prevent its transmission through the fiber when driven with a peak voltage of 25 V. Because the deflection is of the order of the fiber

diameter, the beam cannot propagate through the fiber and extinction will be high. Even with an amplifier-saturating 50 mW, 0.5 mm diameter beam incident on the modulator, the 25 W/cm^2 fluence is still much lower than the 150 kW/cm^2 room temperature damage threshold seen with MgO:SLT and MgO:LN at 532 nm (threshold is lower for shorter wavelengths). Therefore, to answer questions #3 and #4, the production of a low voltage, high extinction, and high damage threshold modulator should be feasible.

The modulator model has shown that it can predict low frequency and static deflections very close to those being measured. From the nonlinear coefficients of the substrates being considered and the geometry of the domains within the engineered crystal, a peak voltage of 25 V is expected to deflect a collimated beam away from the fiber core it is being launched into. Because the modulator crystal is no different from those used by other companies manufacturing amplitude modulators, it is expected that the AdvR-engineered crystal will perform at 100's of MHz like the others. The benefits lie in the modulator scheme – by deflecting the beam away from the core of an optical fiber, bias controls to correct the extinction for ambient drift are not necessary. In addition, the reduced drive voltage means smaller RF amplifiers are required and their associated RFI. By correctly matching the crystal impedance to the RF feedline using known RF design procedures, an efficient and compact, high power, fiber-in, fiber-out amplitude modulator without adjustments can be produced.